# Correlated fermions in nuclei and ultracold atomic gases

O. Hen, L. B. Weinstein, E. Piasetzky, G. A. Miller, M. M. Sargsian, and Y. Sagi

# Correlated Fermion Pairs in Nuclei and Ultracold Atomic Gases

O. Hen,[1, *] L.B. Weinstein,[2] E. Piasetzky,[1] G.A. Miller,[3] M.M. Sargsian,[4] and Y. Sagi[5]

[1]*Tel Aviv University, Tel Aviv 69978, Israel*
[2]*Old Dominion University, Norfolk, VA 23529, USA*
[3]*University of Washington, Seattle, WA 98195-1560, USA*
[4]*Florida International University, Miami, FL 33199, USA*
[5]*Department of Physics, Technion  Israel Institute of Technology, Haifa 32000, Israel*

**Background:** The high momentum distribution of atoms in two spin-state ultra-cold atomic gases with strong short-range interactions between atoms with different spins, which can be described using Tan's contact, are dominated by short range pairs of different fermions and decreases as $k^{-4}$. In atomic nuclei the momentum distribution of nucleons above the Fermi momentum ($k > k_F \approx 250$ Mev/c) is also dominated by short range correlated different-fermion (neutron-proton) pairs.

**Purpose:** Compare high-momentum unlike-fermion momentum distributions in atomic and nuclear systems.

**Methods:** We show that, for $k > k_F$ MeV/c, nuclear momentum distributions are proportional to that of the deuteron. We then examine the deuteron momentum distributions derived from a wide variety of modern nucleon-nucleon potentials that are consistent with $NN$-scattering data.

**Results:** The high momentum tail of the deuteron momentum distribution, and hence of the nuclear momentum distributions appears to decrease as $k^{-4}$. This behavior is shown to arise from the effects of the tensor part of the nucleon-nucleon potential. In addition, when the dimensionless interaction strength for the atomic system is chosen to be similar to that of atomic nuclei, the probability for finding a short range different-fermion pair in both systems is the same.

**Conclusions:** Although nuclei do not satisfy all of the conditions for Tan's contact, the observed similarity of the magnitude and $k^{-4}$ shape of nuclear and atomic momentum distributions is remarkable because these systems differ by about 20 orders of magnitude in density. This similarity may lead to a greater understanding of nuclei and the density dependence of nuclear systems.

**Introduction:** Interacting many-body Fermionic systems are abundant in nature. In non-interacting Fermi systems at zero temperature, the maximum momentum of any Fermion in the system is the Fermi momentum, $k_F$. Independent Fermions moving in a mean field potential have only a small probability to have $k > k_F$. However, an additional short-range interaction between fermions creates a significant high-momentum tail. In this work we discuss two very different systems each composed of two dominant kinds of fermions: protons and neutrons in atomic nuclei and two spin-state ultra-cold atomic gases. While these systems differ by more than 20 orders of magnitude in density, and the fermion-fermion interactions are very different, both exhibit a strong short-range interaction between unlike fermions creating short range correlated (SRC) pairs of unlike fermions that dominate the high momentum tail.

The momentum distribution of a dilute two-component atomic Fermi gas with contact interactions is known to exhibit a $C/k^4$ tail for $k > k_F$, where $C$ is the contact as defined by Tan [1–12]. The value of $C$ depends on the strength of interaction between the two components, as parametrized by $a$, the scattering length. Here we will show that although nuclei do not fulfill the stringent conditions of Tan's relations, their momentum distribution is remarkably similar to that of ultracold Fermi gases with the same dimensionless interaction strength $(k_F a)^{-1}$. The similarity is in both its functional scaling and the spectral weight of the tail.

While this remarkable similarity may be accidental, it is plausible that Fermi systems with a complicated non-contact interaction may still posses universal properties on scales much larger than the scale of the interaction. This approach might lead to greater insight into nuclear pair-correlations as well as the behavior of density dependence of nuclear systems.

This paper is structured as follows: we review our knowledge of nucleon-nucleon pair correlations in nuclei, emphasizing that (1) the momentum distribution of nucleons in nuclei at $k > k_F$ is dominated by proton-neutron ($np$) pairs and (2) the momentum distribution of nucleons in medium to heavy nuclei is proportional to that of the deuteron at high momenta. We then show that (3) the momentum distribution of nucleons in the deuteron and hence in all nuclei decreases approximately as $k^{-4}$ at high momenta, which (4) can be understood from the short distance structure of correlations. This $k^{-4}$ distribution is (5) the same momentum distribution as for the previously measured atoms in ultra-cold two-spin-state atomic gases with a contact interaction. We also show that (6) the pair correlations probability for unlike fermions (i.e., the magnitude of the momentum distribution at high momentum) is the same for nuclei and for atomic systems when the dimensionless interac-

————————
*Contact Author `or.chen@mail.huji.ac.il`

tion strength of the atomic system is chosen to be the same as for nuclei. We then explore (7) the applicability of the conditions of Tan's theory to atomic nuclei. We discuss soft and hard nucleon-nucleon interactions in the Appendix.

Previous papers explored the nuclear momentum distribution as well as relationships between atomic and nuclear systems. Amado and Woloshyn [13] showed that the nuclear momentum distribution $n(k) \propto (k^{-2}v(k))^2$ where $v(k)$ is the fourrier transform of the nucleon-nucleon potential. This decreases as $k^{-4}$ if $v(k)$ is momentum-independent. Sartor and Mahaux found a more complicated form for the momentum distribution at $k > k_F$ for a dilute Fermi gas [14, 15], although their momentum distribution also decreases approximately as $k^{-4}$ for large momenta. Studies of the $^3$He Fermi liquid might also be relevant to this topic [16]. Carlson *et al.* compared quantum monte carlo approaches to neutron matter and atomic physics [17]. Özen and Zinner [18] proposed creating a two-component cold Fermi gas closely analogous to nuclear systems. Zinner and Jensen [19, 20] explored the differences and similarities between nuclei and cold atomic gases. They point out that "As the contact parameters are expected to be universal, they should be the same for a nuclear system in the limit of large scattering length." This work builds on these studies and examines quantitatively the connections and similarities between two-component atomic and nuclear systems. Our analysis is different than recent work that relates the nuclear contact to the Levinger Constant [21].

**(1) Short Range Correlations in Nuclei:** Atomic nuclei are among the most common many-body Fermi-systems. Analysis of electron-nucleus scattering [22] confirmed that medium and heavy nuclei, with atomic weight $A \geq 12$, exhibit the properties of a degenerate system with a characteristic Fermi momentum, $k_F \approx 250$ MeV/c. However, experiments also show that nuclei are not completely described by the independent particle approximation and that, as expected [23, 24], two-particle correlations are a leading correction [25–31]. Nuclei are composed of protons and neutrons with up and down spins, which can create six different types of nucleon pairs. However, isospin invariance reduces the types of independent pairs to four: spin-singlet proton-proton ($pp$), neutron-neutron ($nn$), and proton-neutron ($pn$) pairs and spin-triplet $pn$ pairs. Isospin symmetry further implies that all three types of spin-singlet pairs are similar to each other, reducing the types of pairs to two: spin-singlet and spin-triplet. These pairs have either even or odd values of the orbital angular momentum $L$ according to the generalized Pauli principle, $(-1)^{L+S+T} = -1$.

Experiments show that short-range correlated nucleon-nucleon pairs account for approximately all of the high momentum, $k > k_F$, nucleons in nuclei and about 20–25% of all the nucleons in nuclei [25–31]. They also show that short-range $np$ pairs dominate over $pp$ pairs with a ratio $np/pp = 18 \pm 5$ [29–31], even in heavy asymmetric

nuclei such as lead [32]. As $np$ pairs include contributions from both spin-singlet and spin-triplet pairs whereas $pp$ pairs are entirely spin-singlet, the observed $np/pp$ ratio implies that spin-triplet $np$ pairs account for 85±3% of all pairs with spin-singlet isospin-triplet $pp$, $nn$ and $np$ pairs contributing 5±1% each for a total of 15±3% spin-singlet pairs. This is due to the dominant tensor interaction (which acts only in spin-triplet states) between nucleons at relative momenta between 300 and 600 MeV/c [33–35]. Corrections due to correlations amongst three nucleons or more are small [23, 26] and appear only for nucleon momenta greater than about 800 MeV/c.

**(2) Nuclear momentum distributions:** Because of the observed dominance of $np$ pairs in SRCs we can use the independent-pair approximation [36] to write the momentum density at $k > k_F$ for heavier nuclei as:

$$n_A(k) = a_2(A)n_d(k), \qquad (1)$$

where $n_A(k)$ and $n_d(k)$ are the high momentum parts of the nucleon momentum distribution for a nucleus of atomic number $A$ and deuterium respectively and the factor $a_2(A)$ is independent of $k$ and is the probability of finding a high momentum pair in nucleus $A$ relative to deuterium.

This simple picture was validated experimentally by measurements of the ratios of per-nucleon inclusive electron scattering cross sections for nuclei of atomic number $A$ relative to deuterium at four-momentum transfer squared, $Q^2 = \vec{q}^2 - \omega^2 > 1.5$ GeV$^2$ and Bjorken scaling parameter $1.5 < x < 1.9$ where $x = Q^2/2m\omega$, $\vec{q}$ and $\omega$ are the three-momentum and energy transferred to the nucleus, and $m$ is the nucleon mass. Cross sections in this kinematic region are sensitive to the integral of the nucleon momentum distribution from a threshold momentum to infinity where $k_{thresh} = k_{thresh}(Q^2, x)$ depends on $x$ and $Q^2$ [37]. These cross section ratios are independent of $x$ for $1.5 \leq x \leq 1.9$ and $1.5 \leq Q^2 \leq 3$ GeV$^2$ [25–28], showing that the momentum distributions have similar shapes for approximately $k_F \leq k \lesssim 3k_F$ ($275 \pm 25 \leq k \lesssim 700$ MeV/c) validating Eq. 1. The value of the ratio gives the proportionality constant for the different nuclei

$$a_2(A) = \frac{\sigma_A/A}{\sigma_d/2}. \qquad (2)$$

**(3) Deuteron momentum distributions:** Since the momentum distributions of all nuclei at high momentum are proportional to that of the deuteron for about $k_F \leq k \leq 3k_F$, we now examine the deuteron momentum distribution. We will show that the nucleon momentum distribution for deuterium, and hence for all nuclei, decreases approximately as $k^{-4}$ for the momentum range $1.3\,k_F \leq k \leq 2.5\,k_F$. (In anticipation of the coming discussion of heavy nuclei, we use $k_F = 250$ MeV/c, the typical Fermi momentum for medium and heavy nuclei.)

In order to study the range of possible deuteron momentum distributions, we considered ten modern

nucleon-nucleon ($NN$) potentials that are consistent with the nucleon-nucleon scattering world data set, the Nijmegen 1, 2, and 3 [38], AV18 [39], CD Bonn [40], wjc1 and 2 [41], IIB [42], n3lo500 and n3lo600 [43] nucleon-nucleon interactions.

The chiral effective field theory ($\chi$EFT) N3LO potentials [43] have an explicit momentum cut-off of the form $\exp[-(p/\Lambda)^n]$ where $n = 4, 6$ or 8 and $\Lambda = 500$ or 600 MeV. While we use the N3LO potentials with 500 and 600 MeV cutoffs, the $\chi$EFT neutron-proton phase shifts differ dramatically in some partial waves (especially at higher energy) as the cutoff is varied from 0.7 to 1.5 GeV or as the expansion order is increased from N3LO to N4LO [44]. In addition, "the N2LO, N3LO, and N4LO contributions are all about of the same size, thus raising some concern about the convergence of the chiral expansion for the $NN$-potential [45]." The N5LO contribution is much smaller, indicating convergence [45]. It is unclear how these convergence issues affect the ability of N3LO potentials to describe the high-momentum tail of the deuteron. However, high precision deuteron momentum distributions are not yet available for higher order $\chi$EFT.

There is also some disagreement over the utility of bare interactions versus soft phase-equivalent interactions. This is discussed in detail in the Appendix.

The momentum distribution of a nucleon bound in deuterium, $n_d(k)$, was calculated using each of the modern nucleon-nucleon potentials. The proton and neutron momentum distributions in the deuteron are equal, $n_p(k/k_F) = n_n(k/k_F) = n_d(k/k_F)$, and are normalized so that

$$\frac{1}{(2\pi)^3} \int_0^\infty n(k/k_F)d^3(k/k_F) = 1/2. \qquad (3)$$

We can see the $k^{-4}$ dependence of the momentum distribution clearly in Fig. 1a, which shows the scaled dimensionless momentum distribution, $(k/k_F)^4 n_d(k/k_F)$, for a nucleon bound in deuterium for each of these potentials [43]. We observe $k^{-4}$ scaling in seven of the ten different realistic models, all showing that the ratio

$$R_d = (k/k_F)^4 n_d(k/k_F) = 0.64 \pm 0.10 \qquad (4)$$

for $1.3 \leq k/k_F \leq 2.5$ is constant within about 15% as shown by the red dashed line and uncertainty band in Fig. 1a. Note that $k^{-4}$ changes by a factor of 14 in this range and even the outlying potentials only differ by at most a factor of two from the average.

The experimental reduced $d(e, e'p)$ cross sections for $1.3\,k_F \leq k \leq 2.5\,k_F$ also appear to scale as $k^{-4}$ and provide more evidence for the scaling of the momentum distribution. Fig. 1a also shows the measured $d(e, e'p)$ scaled reduced cross sections, $(k/k_F)^4\sigma_{red}(k/k_F)$, for proton knockout by electron scattering from deuterium in two kinematics where the effects of rescattering of the knocked-out proton (final state interactions or FSI) are expected to be small [46]. The two kinematics are for
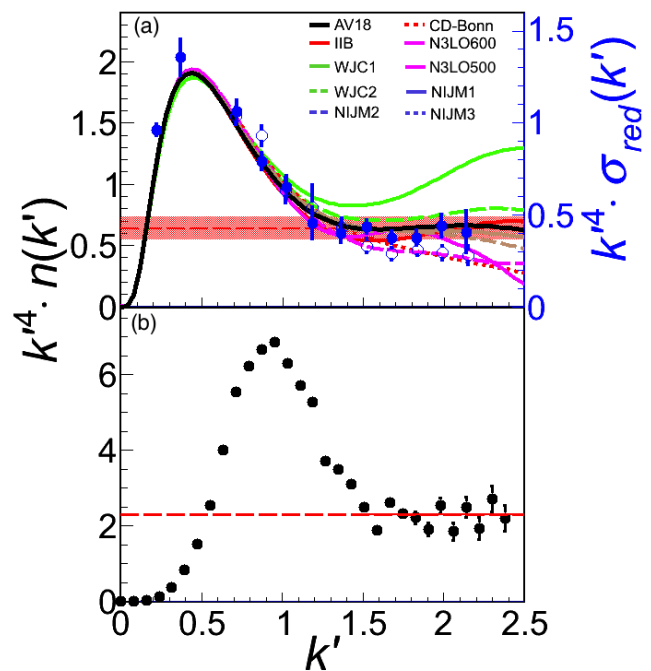


FIG. 1: (color online) The scaled momentum distribution, $k'^4 n(k')$ where $k' = k/k_F$, for deuteron (a) and atomic (b) systems. (a) The curves show the scaled proton momentum distribution for the deuteron calculated from the Nijmegen 1, 2, and 3 [38], AV18 [39], CD Bonn [40], wjc1 and 2 [41], IIB [42], n3lo500 and n3lo600 [43] nucleon-nucleon interactions. The dashed red line is the average of eight of the calculated momentum distributions for $k \geq 1.3k_F$. The red band shows the $\pm 15\%$ uncertainty. The points show the scaled reduced cross sections (using the right-hand $y$-axis), $k'^4\sigma_{red}(k')$, for electron-induced proton knockout from deuterium, $d(e, e'p)$, at $\theta_{nq} = 35°$ (filled circles) and at $\theta_{nq} = 45°$ (open circles)[46]. The curves and points are plotted in units of $k_F = 250$ MeV/c, the typical Fermi momentum for medium and heavy nuclei. This choice of $k_F$ affects the normalization but not the observed $k^{-4}$ scaling. (b) The points show the measured momentum distribution of $^{40}$K atoms in a symmetric two-spin state ultra-cold gas with a short-range interaction between the different spin-states [5]. The dimensionless interaction strength $(k_F a)^{-1} = -0.08 \pm 0.04$. The Fermi momentum is $k_F \approx 1.6$ eV/c.

the angle between the undetected neutron and the momentum transfer, $\theta_{nq} = 35°$ and $45°$. If the electron interacts directly with an on-shell proton and the proton does not rescatter as it leaves the nucleus, then the reduced cross section equals the momentum distribution. Corrections for these effects are model dependent and are on the order of 30–40% (see Ref. [46] and references therein). These effects should be significantly smaller for $\theta_{nq} = 35°$ than for $45°$. The momentum dependence of these effects should also be significantly smaller.

We fitted these momentum distributions by $n_d(k) \propto k^{-\alpha}$ for $1.3k_F \leq k \leq 2.5k_F$ (except for N3LO500 and N3LO600 which we fit up to their cutoffs of 500 MeV/c

($2k_F$) and 600 MeV/c ($2.4k_F$) respectively). We varied the lower and upper fitting bounds by $\pm 0.1k_F$ and $\pm 0.2k_F$ respectively to determine the uncertainty in the exponent $\alpha$ (see Fig. 2). We observe $k^{-4}$ scaling in seven of the ten different realistic models of the nucleon momentum distribution in deuterium.
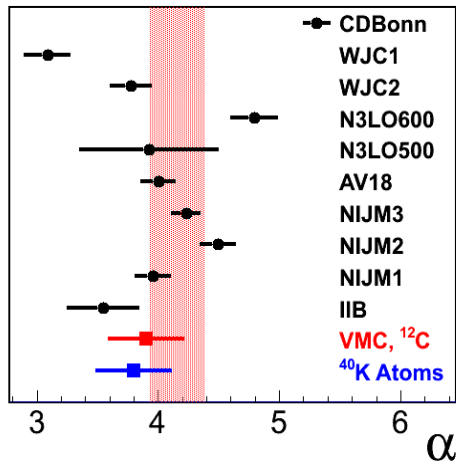


FIG. 2: (color online) The power $\alpha$ obtained by fitting the momentum distribution of the nucleon in deuterium to the form: $n_d(k) \propto k^{-\alpha}$ over $1.3k_F \leq k \leq 2.5k_F$ for the nucleon-nucleon interactions of Fig. 1. The momentum distributions from n3lo500 and n3lo600 are sharply regulated (forced to decrease rapidly) at around 500 ($k = 2k_F$) and 600 MeV/c ($k/k_F = 2.4k_F$) respectively, so we restricted the upper limit of their fit ranges to $2.0k_F$ and $2.4k_F$. The uncertainty of the nuclear momentum distribution exponent comes predominantly from varying the lower and upper bounds of the fitting range by $\pm 0.1k_F$ and $\pm 0.2k_F$ respectively. The red band is the average $\alpha$ ($\pm 2\sigma$) obtained from the deuteron distributions, excluding the two outlier wave-functions: CDBonn and WJC1. Also shown is the result of the power-law fits for the momentum distributions of a nucleon in $^{12}$C [35] and an atom in an ultra-cold two-spin-state $^{40}$K gas [5].

This scaling behavior arises from the sum of the $S$ and $D$ wave contributions to the density. Due to the tensor interaction, the high momentum tail is predominantly produced by $J = 1, S, D$-wave $np$ nucleon pairs ($T = 0, S = 1, L = 0, 2$ or $^3S_1 - ^3D_1$) [47]. For larger momenta, $k > 2.5k_F$, the momentum distribution falls more rapidly with $k$. However, this accounts for less than 1% of the fermions in the system [26]. The momentum distribution of $pp$ pairs does not scale, since there is a minimum in the momentum distribution at $k/k_F \approx 1.6$.

In agreement with the $np$-pair dominance model, exact calculations of the $^{12}$C momentum distribution using the AV18 potential also show $k^{-4}$ scaling [35]. Rios, Polls and Dickhoff calculated the momentum distribution for infinite symmetric nuclear matter using a self-consistent Green's function (SCGF) approach for the AV18, CD-Bonn and N3LO500 interactions [48, 49]. They show that the N3LO500 potential fails to reproduce the measured deuteron momentum distributions. Their AV18 and CD-Bonn nuclear matter momentum distributions decrease with approximately the same exponent $\alpha$ as do the AV18 and CDBonn deuteron momentum distributions shown in Fig. 2.

Based on the inclusive $A(e, e')$ cross section ratios discussed above, the $np$-pair dominance model, and the calculations of nuclear and nuclear matter momentum distributions, we conclude that the momentum distributions of all nuclei decrease approximately as $k^{-4}$.

**(4) Understanding the $k^{-4}$ scaling**: This scaling should not be surprising. Colle et al. [50] found that the nuclear mass dependence of the number of SRC $pp$ and $pn$ pairs in nuclei can be described by tensor operators acting on $NN$ pairs in a nodeless relative $S$-state of the mean-field basis [51]. This very short range behavior of the correlated part of the $NN$ interaction leads to $k^{-4}$ momentum dependence at high momentum, as is shown next.

This $k^{-4}$ behavior can be understood to arise from the importance of the one pion exchange (OPE) contribution to the tensor potential $V_T$, acting in second order. The Schoedinger equation for the spin-one two-nucleon system, which involves $S$ and $D$ state components, can be expressed as an equation involving the $S$ state only by using $(-B - H_0)|\Psi_D\rangle = V_T|\Psi_S\rangle$, where $B$ is the binding energy of the system and $H_0$ is the Hamiltonian excluding the tensor potential. Thus one obtains an effective $S$−state potential: $V_{00} = V_T(-B - H_0)^{-1}V_T$, where $V_T$ connects the $S$ and $D$ states. The intermediate Hamiltonian $H_0$ is dominated by the effects of the centrifugal barrier and can be approximated by the kinetic energy operator. This second-order term is large because it contains an isospin factor $(\tau_1 \cdot \tau_2)^2 = 9$, and because $S_{12}^2 = 8 - 2S_{12}$. Evaluation of the $S$-state potential, neglecting the small effects of the central potential in the intermediate $D$-state, yields

$$V_{00}(k, k') \approx -M\frac{16f^4}{\mu^4\pi^4}\int \frac{p^2pdp}{MB + p^2}I_{02}(k, p)I_{20}(p, k'),$$
(5)

where $M$ is the nucleon mass, $f^2 \approx 0.08$ is the coupling constant, $\mu$ is the pion mass, and $I_{LL'}$ are Fourier transforms of the OPE tensor potential.

$$I_{02}(p, k) = I_{20}(p, k) = \frac{k^2Q_2(z) + p^2Q_0(z)}{2pk} - Q_1(z),$$

with $z \equiv (p^2 + k^2 + \mu^2)/(2pk)$, and $Q_i$ are Legendre functions of the second kind. The important property is that $\lim_{p\to\infty} I_{02}(p, k) = 1 - (k^2 + \mu^2)/p^2 + \cdots$. Thus the integrand of Eq. (5) is dominated by large values of $p$ and diverges unless there is a cutoff. This means that $V_{00}(k', k)$ is approximately a constant, independent of $k$ and $k'$. This is the signature of a short ranged interaction. As discussed in the Introduction, this is the necessary and sufficient condition to obtain an asymptotic two-nucleon wave function $\sim 1/k^2$ and a momentum density $n(k) \sim 1/k^4$. Potentials that do not yield this behavior either have a very weak tensor force or a momentum cutoff at low momenta.

**(5) Comparing the nuclear and atomic high momentum tails:** Fig. 1b shows the $k^{-4}$ scaling of $^{40}$K atoms. Note the remarkable similarity between the data depicted in Fig. 1a and 1b. The nuclear momentum distributions have the same $k^{-4}$ dependence as the momentum distribution measured for two spin-state ultra-cold $^{40}$K atoms of Ref. [5] and as Tan's predictions.

**(6) Nuclear and atomic pair correlations probabilities:** After establishing the similarity in $k^{-4}$ scaling of the momentum distribution tail of the nuclear and cold atoms systems, we now compare the spectral weight contained in these tails. Similar to atomic gases, we define the normalized dimensionless scaling coefficient per particle as

$$\frac{C}{k_F A} \equiv (k/k_F)^4 n(k/k_F) \tag{6}$$

at high momentum, where $A$ is the number of fermions in the system and $n(k/k_F)$ is the dimensionless scaled fermion momentum distribution in units of $k_F$, normalized according to Eq. 3. $C/(k_F A)$ is a measure of the per particle number of short-range correlated pairs. For nuclei

$$\frac{C}{k_F A} = a_2(A) R_d, \tag{7}$$

where $C/(k_F A)$, for nuclei, is the sum of all four possible coefficients, dominated by spin-triplet $np$ pairs, and the ratios $a_2(A)$ are taken from [28]. See Table I.

| Nucleus | $a_2(A)$ | $C/(k_F A)$ |
|---|---|---|
| $^{12}$C | $4.75 \pm 0.16$ | $3.04 \pm 0.49$ |
| $^{56}$Fe | $5.21 \pm 0.20$ | $3.33 \pm 0.54$ |
| $^{197}$Au | $5.16 \pm 0.22$ | $3.30 \pm 0.53$ |

TABLE I: The scaling coefficient extracted for different nuclei. $a_2(A)$ is the ratio of the per nucleon inclusive $(e, e')$ cross sections for nucleus $A$ relative to deuterium for $Q^2 > 1.5$ (GeV/c)$^2$ and $1.5 \leq x \leq 1.9$ [28] (see Eq. 1). $C$ is defined by Eq. 7.

Fig. 3 shows the nuclear coefficients from Table I and the scaled atomic contact as extracted from measurements of the momentum distribution of trapped two spin-state mixtures of ultra-cold $^{40}$K [5] and $^6$Li [6] atomic gases as a function of the dimensionless interaction strength, $(ak_F)^{-1}$. The ultra-cold atomic gas measurements span a wide range of interaction strengths near unitary, in the BCS-BEC crossover regime. In the nuclear case all medium and heavy nuclei are in the unitary regime where $|k_F a|^{-1} \ll 1$, using the typical nuclear Fermi momentum, $k_F = 250$ MeV/c $= 1.27$ fm$^{-1}$ [22] and the $^3S_1$ neutron-proton scattering length, $a = 5.42$ fm [52]. As can be seen, when the dimensionless interaction strength is the same, the scaled atomic contact and the nuclear coefficient agree remarkably well. The integral of the $k^{-4}$ tail of the momentum density is about 0.2.
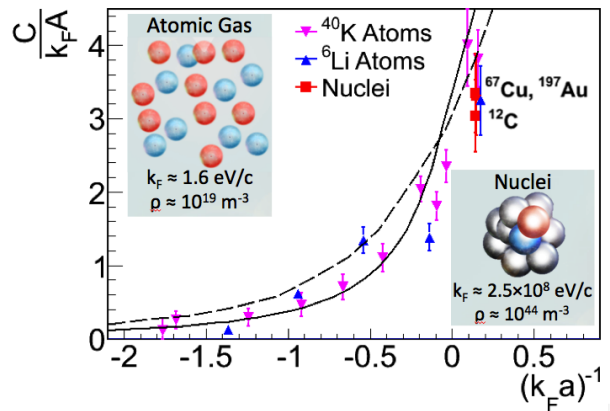


FIG. 3: (color online) The magenta inverted and blue upright triangles show the scaled contact plotted versus $(k_F a)^{-1}$, the inverse of the product of the scattering length and Fermi momentum, as extracted from measurements of ultra-cold two-spin state atomic systems at finite temperature [5, 6]. The red squares show the equivalent coefficient extracted from atomic nuclei (see Table I), which are essentialy at zero temperature. The dashed and solid lines show the theoretical predictions of Refs. [8] and [53] respectively for atomic systems at zero temperature.

Thus, each fermion has a $\approx 20\%$ probability of belonging to a high-momentum different-fermion pair in both the atomic and nuclear systems.

This agreement between the shape and magnitude of the momentum distributions between such wildly disparate systems is remarkable. We now look for the underlying reasons for this agreement.

**(7) Possible Connections to Tan's Contact:** Tan [1–3] and later others [4], showed that a short-range interaction between two different Fermion types leads to a high-momentum tail that falls as $k^{-4}$ (where $k$ is the fermion momentum), and derived a series of universal relations that relate the contact (i.e. the number of short-range correlated pairs) to various thermodynamic properties of the system such as the total energy and pressure. These were recently validated experimentally in ultra-cold two-spin states atomic gas systems [5, 6], see [4] for a review.

Tan obtained relations for dilute systems with scattering length, $a$, and the inter-fermion distance, $d$, which are much larger than the range of the interaction, $r_0$: $a \gg r_0$ and $d \gg r_0$. In such systems the $k^{-4}$ scaling of the momentum distribution is only expected for $ka \gg 1$ and $kr_0 \ll 1$.

As we have shown, atomic nuclei exhibit some of the same key properties as cold atomic Fermi systems. They are characterized by a Fermi momentum $k_F$, and have a strong short-range interaction between (spin-triplet) unlike fermions. The nuclear momentum distributions also fall as $k^{-4}$ for $300 \leq k \leq 600$ MeV/c.

However, unlike systems of atoms, atomic nuclei are self-bound. The nucleon-nucleon force provides both the long range interactions that cause atomic nuclei to resem-

ble Fermi gases and the short-range interaction between fermions. The binding interaction arises in part from the iterated effects of the long-distance one-pion exchange potential and has a range of about $r_0^{bind} \approx \hbar/(m_\pi c) \approx 1.4$ fm, where $m_\pi = 140$ MeV/c$^2$ is the pion mass. The range of the short-range part of the nucleon-nucleon interaction responsible for the spin-triplet $pn$ pairs in the high momentum tail is less well defined. The $NN$-pairs in a nodeless relative $S$-state [50] are at much closer distances than typical nucleons. Similarly, the second-order action of the tensor interaction described in Eq. 5 also must have an effective range much shorter than the long distance pion exchange that binds the nucleus. Quantitatively, various tensor correlation functions shown in [54] peak at an internucleon distance of about 1 fm, so we will estimate that $r_0 \approx 1$ fm. The typical distance between same-type nucleons in nuclei is $d = (\rho_0/2)^{-1/3} \approx 2.3$ fm, where $\rho_0 \approx 0.17$ nucleons/fm$^3$ is the saturation nuclear density. The nucleon-nucleon scattering length in the $^3S_1$ channel is $5.424 \pm 0.003$ fm [52].

Therefore, for nuclei both the interaction length and the inter-nucleon distance are greater, but not much greater, than the range of the short-distance interaction (i.e. $a \approx 5.4\,\text{fm} > d \approx 2\,\text{fm} > r_0 \approx 1\,\text{fm}$). Other required conditions for $1/k^4$ scaling are $k \gg 1/a \approx 40$ MeV/c and $k \ll 1/r_0 \approx 200$ MeV/c for $r_0 \approx 1$ fm. As can be seen in Fig. 1a, scaling occurs for $300 \leq k \leq 600$ MeV/c, much greater than the lower limit of 40 MeV/c. However, $k$ is definitely not much less (or even less) than the upper limit of 200 MeV/c.

The required kinematic conditions discussed above are sufficient, but perhaps not necessary. The scaling of quark distributions measured in deep inelastic electron scattering was observed at momentum transfers much below that expected. This is referred to as 'precocious scaling' [55]. Additionally the $1/k^4$ tail in ultracold Fermi gases was experimentally observed to start at a much lower momentum than predicted [5, 56].

Our extraction is different than a recent work by Weiss, Bazak, and Barnea [21] that relates the nuclear contact term to the Levinger constant. They attempt to extract it from photodisintegration data, which are driven by the electric dipole operator that operates on neutron-proton pairs. Photodisintegration is not a measure of the ground-state nucleon momentum density. Furthermore their analysis is restricted to photon energies below 140 MeV, which corresponds to wavelengths $\lambda \geq 2\pi\hbar c/E = 8.8$ fm which sample the entire nucleus and are not short-range. Also, these photon energies correspond to nucleon momenta less than about 340 MeV/c ($\approx 1.35 k_F$). This is below the $k^{-4}$ scaling region shown in Fig. 1 above. Their average contact (singlet plus triplet over two) equals our triplet contact alone, so that their total contact is double ours and also double that of an atomic system with the same value of $k_F a$.

**Summary:** We have shown that the momentum distribution of nucleons in nuclei for $k > k_F$ is dominated by spin-triplet $pn$ pairs and falls approximately as $k^{-4}$. This is very similar to the momentum distribution of two spin-state ultra-cold atomic gases with a strong short-range interaction between atoms in the different spin states. Remarkably, despite a 20-order-of-magnitude difference in density, when both systems have the same dimensionless interaction strength, $(k_F a)^{-1}$, the magnitudes of the momentum distributions are also equal, indicating that Fermions in the two systems have equal probabilities to belong to correlated pairs.

This leads to the question of whether this agreement between atomic and nuclear systems at remarkably different length, energy and momentum scales is accidental or has a deeper reason. If the agreement has a deeper reason, then perhaps relations like Tan's can be developed for atomic nuclei and a better extrapolation to supradense nuclear systems may be possible.

## I. APPENDIX: SOFT AND HARD $NN$ INTERACTIONS

Nuclear theory must describe a broad range of phenomena from low energies to high energies and from low momentum transfer to high momentum transfer. Therefore one must contend with the fact that the general baryon-baryon interaction includes matrix elements that connect low relative momenta to high relative momenta. These terms can be handled by using so-called soft $NN$ potentials and by generating soft phase-equivalent effective interactions obtained from the bare interactions by means of unitary transformations [57–63].

Calculations of low-energy and low-momentum processes are indeed simplified by using soft interactions, and it is reasonable to obtain such interactions using a unitary transformation. A consistent application of this idea involves transforming the Hamiltonian and all other operators, especially including the currents that account for interactions with external probes [63]. Such transformation are known to convert single-nucleon operators into multi-nucleon operators. The effect on long-range operators such as the radius or electromagnetic transition operators is small [62, 63]. However, the effect on short-range or high-momentum observables is large [63].

To posit the soft-interaction to be the fundamental bare interaction is to deny the reality of high momentum transfer processes. Therefore, the fundamental bare interaction must allow high-momentum transfer processes.

In particular, consider that two-body densities in co-ordinate space have a correlation "hole" near $r = 0$. By transforming only the Hamiltonian and not the two-body density, these correlation holes disappear [63]. Similarly, these Hamiltonian-only transformations dramatically reduce the high-momentum part of the momentum density.

As an example, consider coherent neutrino-nuclear interactions [64–66]. The neutrino interacts weakly and the cross section is proportional to the square of the elastic nuclear form factor. Following [66] we note that the neutrino-nucleus elastic-scattering cross section $d\sigma/d\Omega$ is [67, 68],

$$\frac{d\sigma}{d\Omega} = \frac{G^2}{16\pi^2}k^2(1 + \cos\theta)F^2(Q^2),\qquad(8)$$

for a neutrino of energy $k$ scattering at angle $\theta$, and $G$ is the Fermi coupling constant. The ground-state elastic form factor $F(Q^2)$ at momentum transfer $Q$, $Q^2 = 2k^2(1-\cos\theta)$, is the matrix element of the single-nucleon operator $e^{i\mathbf{q}\cdot\mathbf{r}_i}$, for a nucleon $i$ weighted by the weak charge of the proton or neutron. One could ideally contemplate probing the high-momentum components of nuclear wave functions using neutrino-nuclear interactions. Now imagine that one wished to describe the nuclear wave function using soft interactions. The necessary unitary transformation would transform the simple single-nucleon operator $e^{i\mathbf{q}\cdot\mathbf{r}_i}$, into a complicated multi-body operator, which would ruin the simplicity of using the neutrino as a probe.

If one wishes to use simple probes to investigate high-momentum aspects of nucleon structure, it is necessary to start with a theory involving bare interactions, which are necessarily hard interactions.

[1] S. Tan, Annals of Physics **323**, 2952 (2008).
[2] S. Tan, Annals of Physics **323**, 2971 (2008).
[3] S. Tan, Annals of Physics **323**, 2987 (2008).
[4] E. Braaten, in *The BCS-BEC Crossover and the Unitary Fermi Gas*, edited by W. Zwerger (Springer, Berlin, 2012).
[5] J. T. Stewart, J. P. Gaebler, T. E. Drake, and D. S. Jin, Phys. Rev. Lett. **104**, 235301 (2010).
[6] E. D. Kuhnle, H. Hu, X.-J. Liu, P. Dyke, M. Mark, P. D. Drummond, P. Hannaford, and C. J. Vale, Phys. Rev. Lett. **105**, 070402 (2010).
[7] G. Partridge, K. Strecker, R. Kamar, M. Jack, and R. Hulet, Phys. Rev. Lett. **95**, 020404 (2005).
[8] F. Werner, L. Tarruell, and Y. Castin, The European Physical Journal B **68**, 401 (2009), ISSN 1434-6028.
[9] A. Schirotzek, Ph.D. thesis, Massachusetts Institute of Technology (2010).
[10] Y. Sagi, T. Drake, R. Paudel, and D. Jin, Phys. Rev. Lett. **109**, 220402 (2012).
[11] S. Gandolfi, K. E. Schmidt, and J. Carlson, Phys. Rev. A **83**, 041601 (2011).
[12] S. Hoinka, M. Lingham, K. Fenech, H. Hu, C. J. Vale, J. E. Drut, and S. Gandolfi, Phys. Rev. Lett. **110**, 055305 (2013).
[13] R. Amado and R. Woloshyn, Physics Letters B **62**, 253 (1976), ISSN 0370-2693, URL http://www.sciencedirect.com/science/article/pii/0370269376900678.
[14] R. Sartor and C. Mahaux, Phys. Rev. C **21**, 1546 (1980).
[15] R. Sartor and C. Mahaux, Phys. Rev. C **25**, 677 (1982).
[16] F. Mazzanti, A. Polls, J. Boronat, and J. Casulleras, Phys. Rev. Lett. **92**, 085301 (2004), URL http://link.aps.org/doi/10.1103/PhysRevLett.92.085301.
[17] J. Carlson, S. Gandolfi, and A. Gezerlis, Prog. Theor. Exp. Phys. **01A**, 209 (2012).
[18] C. Ozen and N. T. Zinner, Eur. Phys. J. D **68**, 225 (2014).
[19] N. T. Zinner and A. S. Jensen, Journal of Physics: Conference Series **111**, 012016 (2008), URL http://stacks.iop.org/1742-6596/111/i=1/a=012016.
[20] N. T. Zinner and A. S. Jensen, Journal of Physics G: Nuclear and Particle Physics **40**, 053101 (2013), URL http://stacks.iop.org/0954-3899/40/i=5/a=053101.
[21] R. Weiss, B. Bazak, and N. Barnea, Phys. Rev. Lett. **114**, 012501 (2015).
[22] E. J. Moniz, I. Sick, R. R. Whitney, J. R. Ficenec, R. D. Kephart, and W. P. Trower, Phys. Rev. Lett. **26**, 445 (1971).
[23] H. Bethe, Ann.Rev.Nucl.Part.Sci. **21**, 93 (1971).
[24] L. L. Frankfurt and M. I. Strikman, Phys. Rep. **76**, 215 (1981).
[25] K. Egiyan et al. (CLAS Collaboration), Phys. Rev. C **68**, 014313 (2003).
[26] K. Egiyan et al. (CLAS Collaboration), Phys. Rev. Lett. **96**, 082501 (2006).
[27] L. Frankfurt, M. Strikman, D. Day, and M. Sargsyan, Phys. Rev. C **48**, 2451 (1993).
[28] N. Fomin et al., Phys. Rev. Lett. **108**, 092502 (2012).
[29] E. Piasetzky, M. Sargsian, L. Frankfurt, M. Strikman, and J. W. Watson, Phys. Rev. Lett. **97**, 162504 (2006).
[30] R. Subedi et al., Science **320**, 1476 (2008).
[31] I. Korover, N. Muangma, O. Hen, et al., Phys.Rev.Lett. **113**, 022501 (2014), 1401.6138.
[32] O. Hen et al. (CLAS Collaboration), Science **346**, 614 (2014).
[33] M. M. Sargsian, T. V. Abrahamyan, M. I. Strikman, and L. L. Frankfurt, Phys. Rev. C **71**, 044615 (2005).
[34] R. Schiavilla, R. B. Wiringa, S. C. Pieper, and J. Carlson, Physical Review Letters **98**, 132501 (2007).
[35] R. B. Wiringa, R. Schiavilla, S. C. Pieper, and J. Carlson, Phys. Rev. C **89**, 024305 (2014).
[36] A. de Shalit and H. Feshbach, *Theoretical Nuclear Physics, Volume I: Nuclear Structure* (John Wiley & Sons, INC, New York, 1974), ISBN O-471-20385-8.
[37] J. Arrington, D. Higinbotham, G. Rosner, and M. Sargsian, Prog.Part.Nucl.Phys. **67**, 898 (2012), 1104.1196.
[38] V. G. J. Stoks, R. A. M. Klomp, C. P. F. Terheggen, and J. J. de Swart, Phys. Rev. C **49**, 2950 (1994).

[39] R. B. Wiringa, V. G. J. Stoks, and R. Schiavilla, Phys. Rev. C **51**, 38 (1995).

[40] R. Machleidt, Phys. Rev. C **63**, 024001 (2001).

[41] F. Gross and A. Stadler, Few-Body Systems **44**, 295 (2008), ISSN 0177-7963.

[42] F. Gross, J. W. Van Orden, and K. Holinde, Phys. Rev. C **45**, 2094 (1992).

[43] R. Machleidt and D. Entem, Physics Reports **503**, 1 (2011), ISSN 0370-1573.

[44] D. R. Entem, N. Kaiser, R. Machleidt, and Y. Nosyk, Phys. Rev. C **91**, 014002 (2015).

[45] D. R. Entem, N. Kaiser, R. Machleidt, and Y. Nosyk, *Dominant contributions to the nucleon-nucleon interaction at sixth order of chiral perturbation theory* (2015), 1505.03562.

[46] W. Boeglin et al. (Hall A Collaboration), Phys.Rev.Lett. **107**, 262501 (2011).

[47] M. Vanhalst, W. Cosyn, and J. Ryckebusch, *Stylized features of single-nucleon momentum distributions* (2014), 1405.3814.

[48] A. Rios, A. Polls, and W. H. Dickhoff, Phys. Rev. C **79**, 064308 (2009).

[49] A. Rios, A. Polls, and W. H. Dickhoff, Phys. Rev. C **89**, 044303 (2014).

[50] C. Colle et al., Phys. Rev. C **92**, 024604 (2015).

[51] J. Ryckebusch, M. Vanhalst, and W. Cosyn, Journal of Physics G: Nuclear and Particle Physics **42**, 055104 (2015), URL http://stacks.iop.org/0954-3899/42/i=5/a=055104.

[52] L. Koester and W. Nistler, Z. für Physik A pp. 189–196 (1975).

[53] R. Haussmann, M. Punk, and W. Zwerger, Phys. Rev. A **80**, 063612 (2009).

[54] M. Vanhalst, J. Ryckebusch, and W. Cosyn, Phys. Rev. C **86**, 044619 (2012).

[55] H. Georgi and H. D. Politzer, Phys. Rev. Lett. **36**, 1281 (1976).

[56] H. Hu, X.-J. Liu, and P. D. Drummond, New J.Phys. **13**, 035007 (2011), 1011.3845.

[57] S. Bogner, T. Kuo, and A. Schwenk, Physics Reports **386**, 1 (2003), ISSN 0370-1573, URL http://www.sciencedirect.com/science/article/pii/S0370157303002953.

[58] H. Feldmeier, T. Neff, R. Roth, and J. Schnack, Nuclear Physics A **632**, 61 (1998), ISSN 0375-9474, URL http://www.sciencedirect.com/science/article/pii/S0375947497008051.

[59] R. Roth, T. Neff, and H. Feldmeier, Progress in Particle and Nuclear Physics **65**, 50 (2010), ISSN 0146-6410, URL http://www.sciencedirect.com/science/article/pii/S0146641010000335.

[60] S. K. Bogner, R. J. Furnstahl, and R. J. Perry, Phys. Rev. C **75**, 061001 (2007), URL http://link.aps.org/doi/10.1103/PhysRevC.75.061001.

[61] S. Bogner, R. Furnstahl, and A. Schwenk, Progress in Particle and Nuclear Physics **65**, 94 (2010), ISSN 0146-6410, URL http://www.sciencedirect.com/science/article/pii/S0146641010000347.

[62] K. A. Wendt, R. J. Furnstahl, and R. J. Perry, Phys. Rev. C **83**, 034005 (2011), URL http://link.aps.org/doi/10.1103/PhysRevC.83.034005.

[63] T. Neff, H. Feldmeier, and W. Horiuchi, Phys. Rev. C **92**, 024003 (2015), URL http://link.aps.org/doi/10.1103/PhysRevC.92.024003.

[64] K. Scholberg, Phys. Rev. D **73**, 033005 (2006), URL http://link.aps.org/doi/10.1103/PhysRevD.73.033005.

[65] D. Akimov et al. (2013), 1310.0125 [hep-ex].

[66] C. J. Horowitz, K. J. Coakley, and D. N. McKinsey, Phys. Rev. D **68**, 023005 (2003), URL http://link.aps.org/doi/10.1103/PhysRevD.68.023005.

[67] D. Z. Freedman, D. N. Schramm, and D. L. Tubbs, Ann. Rev. Nucl. Sci. **27**, 167 (1977).

[68] A. Drukier and L. Stodolsky, Phys. Rev. D **30**, 2295 (1984), URL http://link.aps.org/doi/10.1103/PhysRevD.30.2295.